Appendix C

Sample Laboratory Report

Lamina Tensile Response

The lamina tensile response of a carbon–fiber, epoxy–matrix composite was examined experimentally to establish the intrinsic mechanical properties. The test specimen geometries were chosen according to the outline presented in Chapter 5, in accordance with ASTM standards. The specimens were loaded to failure in a tensile testing machine utilizing serrated wedge grips. Average test results and standard deviations were as follows:

Elastic modulus in the fiber direction		$E_1 = 126 \pm 2$ GPa
Elastic modulus transverse to the fiber direction		$E_2 = 10.2 \pm 0.4$ GPa
Poisson's ratios:	Major	$\nu_{12} = 0.30 \pm 0.01$
	Minor	$\nu_{21} = 0.024$
Ultimate tensile stress in the fiber direction		$X_1^T = 2037 \pm 85$ MPa
Ultimate tensile stress in the transverse direction		$X_2^T = 53 \pm 8$ MPa
Ultimate tensile strain in the fiber direction		$e_1^T = 0.015$
Ultimate tensile strain in the transverse direction		$e_2^T = 0.0057$

Procedure

The procedure for this experiment is detailed in Chapter 5. Briefly, unidirectional panels were configured for achieving test specimens with 0 and 90° orientation as shown in Appendix B. After the edges of the panels were trimmed, tabs made from a glass–fabric epoxy laminate were adhesively bonded to both surfaces at two opposite edges of the panels. Four specimens of each orientation were machined to the appropriate widths using procedures detailed in Chapter 4. The 0° specimens were nominally 12.7 mm wide, whereas the 90° specimens were 25.4 mm wide. The 0° specimens were 8 plies thick, whereas the 90° specimens were 16 plies thick. To establish the axial stiffness (E_1), Poisson's ratio (ν_{12}), and the overall stress–strain response of the 0° specimens, a bidirectional (0°/90°) strain gage rosette was bonded at the geometric center on one surface of each specimen. In addition, an axial gage was bonded on the opposite surface of the specimen. For the 90°

specimens, a single-element strain gage oriented along the length of the specimen was bonded to each surface of the specimen in the gage section to determine the axial stress–strain response. No strain gages transverse to the specimen loading axis were used because the minor Poisson's ratio (ν_{21}) may be determined from E_1, E_2, and ν_{12}. Each specimen was tested in a general-purpose testing machine at a crosshead rate of 2 mm/min. Specimen load and strains were sampled throughout the test using a PC-driven data acquisition system. The specimens were loaded to failure.

Specimen Dimensions

Specimen cross-sectional dimensions were recorded as follows:

Specimen	Orientation (deg)	Width (w) (mm)	Thickness (t) (mm)
1	0	12.78	1.067
2	0	12.78	1.067
3	0	12.65	1.067
4	0	12.75	1.067
5	90	25.40	2.184
6	90	25.35	2.185
7	90	25.45	2.134
8	90	25.53	2.236

Stress–Strain Data

The load readings were converted to axial stress readings using the cross-sectional dimensions reported above. Examples of stress and strain data recorded using the data acquisition system are tabulated below.

Stress-Strain Data for Specimen 2 ($[0]_8$) (Reduced Set from Original Record)
The last two columns are strain readings from the same strain gage rosette.

σ_1 (MPa)	ε_1 (μstrain)	ε_1 (μstrain)	$-\varepsilon_2$ (μstrain)
0	0	10	0
36	310	320	120
72	590	600	200
108	860	870	280
144	1,140	1,160	340
180	1,420	1,440	420
252	2,010	2,000	570
395	3,050	3,030	880
647	4,900	4,850	1,380
1,006	7,490	7,430	2,040
1,294	9,470	9,420	2,540
1,617	11,640	11,590	3,070
1,977[a]	14,060	13,990	3,610

[a] Ultimate stress.

Stress-Strain Data for Specimen 6 ($[90]_{16}$)
(Reduced Set from Original Record)

σ_2 (MPa)	ε_2 (μstrain)	ε_2 (μstrain)
0	0	0
1.77	180	200
3.54	350	380
5.31	520	550
10.6	1040	1120
17.7	1750	1860
23.0	2290	2410
30.1	2990	3130
35.4	3520	3690
40.7	4120	4330
49.6	5050	5280
60.2	6220	6510
63.4[a]	6580	6879

[a] Ultimate stress.

Test Results

Test results for three representative 0° test specimens are presented in graphical form in Figures C.1–C.3. The linear response region in the fiber direction is bounded by a strain of about 0.004. It is noteworthy that the stress–strain response exhibits strain hardening characteristics — a reflection of the strain hardening behavior of carbon fibers. Results for three representative 90° specimens are shown in Figures C.4–C.6. Here only a modest nonlinearity in the stress–strain response is observed. The strain softening is due to the nonlinear response of the epoxy matrix.

Reduced Data

The mechanical properties were reduced from the measured data using procedures and equations provided in Chapter 5. The following equations were employed:

$$E_1 = \frac{\sigma_1}{\varepsilon_1} \tag{C.1}$$

$$\upsilon_{12} = \frac{-\varepsilon_2}{\varepsilon_1} \tag{C.2}$$

$$X_1^T = \sigma_1^{ult} \tag{C.3}$$

$$E_2 = \frac{\sigma_2}{\varepsilon_2} \tag{C.4}$$

$$X_2^T = \sigma_2^{ult} \tag{C.5}$$

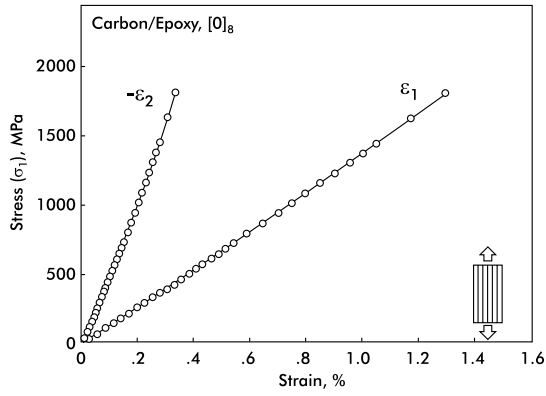

FIGURE C.1
Stress–strain results for specimen 1 (0°).

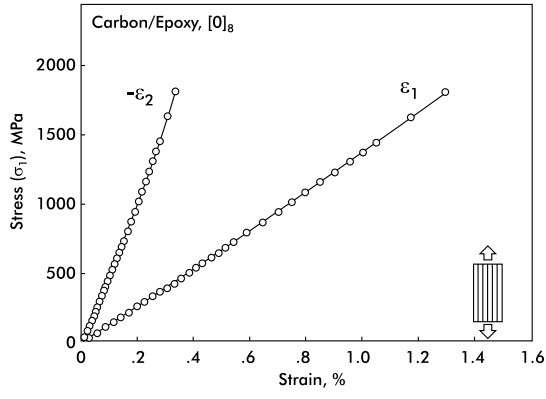

FIGURE C.2
Stress–strain results for specimen 2 (0°).

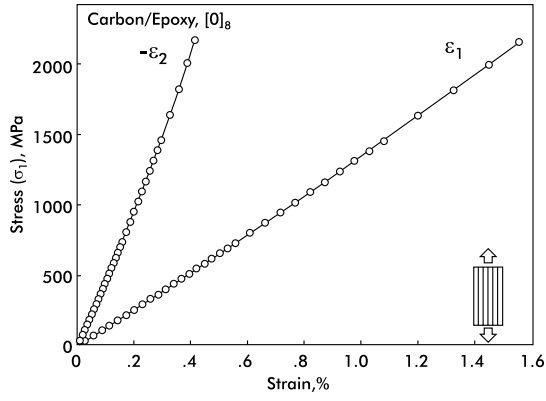

FIGURE C.3
Stress–strain results for specimen 3 (0°).

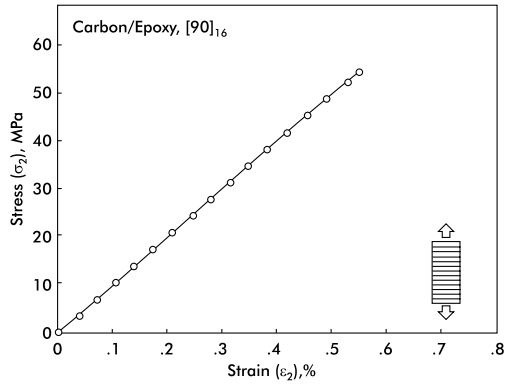

FIGURE C.4
Stress–strain results for specimen 5 (90°).

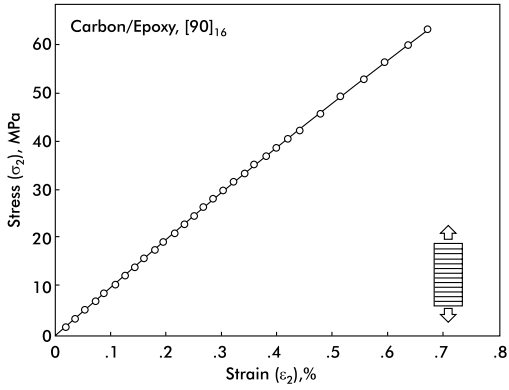

FIGURE C.5
Stress–strain results for specimen 6 (90°).

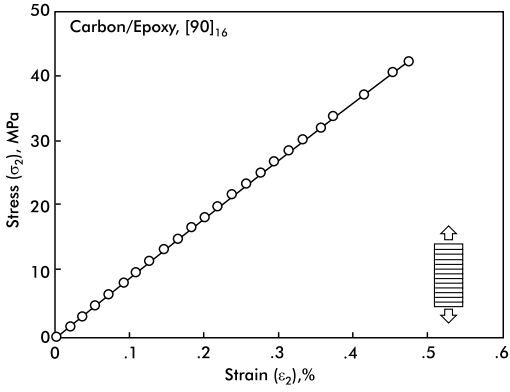

FIGURE C.6
Stress–strain results for specimen 7 (90°).

where σ_1 and σ_2 refer to the load per unit cross-sectional area ($\sigma = P/(wt)$) for the 0 and 90° tests, respectively. Note that it was not possible to evaluate experimentally the minor Poisson's ratio, ν_{21}, because the 90° specimens were not instrumented with a transversely oriented strain gage. The reduced data are summarized below.

	E_1 (GPa)	ν_{12}	X_1^T (MPa)	e_1^T	E_2 (GPa)	X_2^T (MPa)	e_2^T
	128	0.295	2034	0.015	9.92	54.5	0.0056
	127	0.292	1800	0.013	9.79	63.4	0.0067
	124	0.299	2158	0.016	10.5	45.6	0.0046
	125	0.319	1979	0.014	10.4	48.3	0.0049
Avg.	126	0.301	1993	0.015	10.2	53.0	0.0055
STD[a]	2	0.012	149	0.001	0.4	7.9	0.0010

[a] STD = standard deviation.

Using the reciprocal relations between the elastic moduli and Poisson's ratios given in Chapter 2, the minor Poisson's ratio was determined as

$$\nu_{21} = \nu_{12}E_2/E_1 = 0.301 \times 10.2/126 = 0.024$$

Uncertainty Analysis

An uncertainty analysis was performed to estimate the possible scatter range in the mechanical properties as a result of uncertainties in the primary measurements of force, strain, and specimen dimensions. Procedures for such estimation are outlined in the text by Holman and Gajda [1]. Here, we will perform a simple, conservative propagation of error analysis [1] on the governing Equations (C.1–C.5) used for data reduction and property determination. Such an analysis yields

$$\Delta E_i = E_i\left[\frac{\Delta P}{P} + \frac{\Delta w}{w} + \frac{\Delta t}{t} + \frac{\Delta \varepsilon}{\varepsilon}\right] \qquad i = 1,2 \tag{C.6}$$

$$\Delta \upsilon_{12} = \upsilon_{12}\left[\frac{\Delta \varepsilon_1}{\varepsilon_1} + \frac{\Delta \varepsilon_2}{\varepsilon_2}\right] \tag{C.7}$$

$$\Delta X_i^T = X_i^T\left[\frac{\Delta P}{P} + \frac{\Delta w}{w} + \frac{\Delta t}{t}\right] \qquad i = 1,2 \tag{C.8}$$

Consider the uncertainties in measuring the load (P), strain (ε), and dimensions (w and t):

$$\Delta P = \pm 10N$$

$$\Delta \varepsilon = \pm 5 \times 10^{-6}$$

$$\Delta w = \pm 0.025 \text{ mm}$$

$$\Delta t = \pm 0.025 \text{ mm}$$

With the above uncertainties in the load and strain data and in the cross-sectional dimensions, load and strain values were inserted into Equations (C.6)-(C.8) to yield the uncertainties in the reduced mechanical properties. When considering uncertainties in the elastic moduli (E_i) and Poisson's ratio (ν_{12}), the load and strains in the middle of the linear response region (Figures C.1–C.6) were used. For uncertainty analysis of the strengths (X_i^T), the ultimate loads were used. The calculations yield the following uncertainties:

$$\Delta E_1 = 3.2 \text{ GPa}$$

$$\Delta \nu_{12} = 0.002$$

$$\Delta X_1^T = 52 \text{ MPa}$$

$$\Delta E_2 = 0.3 \text{ GPa}$$

$$\Delta X_2^T = 1.0 \text{ MPa}$$

The uncertainties are all below 4% of the corresponding average values, which indicates that the measuring accuracy was reasonable. For several of the mechanical properties the standard deviation exceeds the above-estimated uncertainties, which indicates that the variability of the material properties contributes to the scatter.

Micromechanics Predictions

It is useful to compare the measured properties to those predicted by the micromechanics analyses discussed in Chapter 2. Previous laboratory experiments using an AS4/3501-6 carbon/epoxy composite gave a fiber volume fraction of 0.55 (see Chapter 3). Application of the micromechanics relations for E_1, ν_{12}, and E_2 given in Chapter 2, i.e., Equations (2.25a), (2.25c), and (2.26), together with the following data for AS4 carbon fibers and 3501-6 epoxy obtained from References [2–4]:

Fiber Data [2,3]	Matrix Data [3,4]
Axial modulus (E_L), 235 GPa	Young's modulus (E), 4.28 GPa
Transverse modulus (E_T), 13.8 GPa	Poisson's ratio (ν), 0.35
Axial Poisson's ratio (ν_{LT}), 0.20	

yields the following estimate of the mechanical properties of the composite

$$E_1 = 131 \text{ GPa}$$

$$\nu_{12} = 0.27$$

$$E_2 = 8.3 \text{ GPa}$$

The estimated properties agree reasonably well with the measured data. The differences may be due to variations in fiber volume fraction.

References

1. J.P. Holman and W.J. Gajda, Jr., *Experimental Methods for Engineers*, 5th ed., McGraw-Hill, New York, 1993.
2. Product Data, Number 841-4, Hercules Inc., Wilmington, DE, 1987.
3. J. Aboudi, *Mechanics of Composite Materials — A Unified Micromechanical Approach*, Studies in Applied Mechanics - 29, Elsevier, Amsterdam, 1991.
4. N.J. Johnston, T.W. Towell, and P.M. Hergenrother, Physical and mechanical properties of high-performance thermoplastic polymers and their composite materials, in *Thermoplastic Composite Materials*, L.A. Carlsson, ed., Elsevier, Amsterdam, 1991, pp. 27–71.